

Interference Suppression in Ultra-Wideband Communications

Li Zhao and Alexander M. Haimovich¹
 Department of Electrical and Computer Engineering
 New Jersey Institute of Technology
 Newark, New Jersey 07102, USA
 e-mail: lxz0111@oak.njit.edu, haimovic@njit.edu

Abstract — In this paper we analyze the performance of ultra-wideband (UWB) communications in the presence interference. The interference is modeled as a zero mean random process with constant power spectral density over a certain bandwidth. Mathematical expressions are developed for the *jam resistance* of a pulse position modulation UWB utilizing a Gaussian monocycle. We also compare the interference suppression properties of UWB with those of direct-sequence spread spectrum (DS-SS). It is shown that under certain assumptions UWB provides more effective interference suppression than DS-SS.

I. INTRODUCTION

The increased depletion of the frequency spectrum due to soaring wireless applications calls for the development of new efficient wireless technologies. The existing paradigm of portions of the spectrum allocated to specific applications, such that significant portions of the spectrum are tied up even when the traffic is light, is not efficient. There is a growing interest in communications techniques that can share the spectrum with existing applications. One such technique is based on the transmission of ultra-wideband (UWB) signals with very low power spectral density. Interest in UWB technology has been further heightened by a recent FCC announcement of notice of proposed rulemaking concerning UWB usage, issued May 10, 2000.

UWB has its beginnings in radar and it is also known as *impulse radio* [1, 2]. Unlike conventional wireless communications systems that are carrier-based, UWB-based communications is baseband. It uses a series of short pulses that spread the energy of the signal from near DC to a few GHz. One typical technique is to assign a window in time and shift the position of the pulse within that window. This is classical pulse position modulation (PPM). Since gigahertz unoccupied slices of bandwidth are not available at microwave frequencies, under FCC regulations, UWB radio must be treated as spurious interference to all other communication systems. In addition, UWB radios operating over the densely populated frequency range below a few gigahertz, must contend with a variety of interfering signals. This important feature hints to the similarities between UWB and conventional spread spectrum technologies such as direct-sequence spread spectrum.

Similar to UWB systems, spread spectrum communications systems have their beginnings in military applications due to: (1) their jam resistance capabilities and (2) low power spectral density, which makes them difficult to detect/intercept by an unintended listener. Recent results show that UWB signals

have a lower detectability distance than certain commercial-off-the-shelf (COTS) spread spectrum systems with similar observation intervals, thus making UWB more covert than existing COTS systems [3]. Similarly, we will show in this work that UWB also have jam resistance capabilities superior to other spread spectrum techniques.

The interference suppression ability is measured in terms of the processing gain defined in this context as the ratio of output to input signal-to-interference ratios (SIR). In this paper, we are concerned with analyzing jam resistance properties of UWB systems and comparing them to those of direct-sequence spread spectrum (DS-SS). In both UWB and DS-SS systems, the processing gain is obtained as a result of non-linear filtering operations. With traditional DS-SS, the wide bandwidth is achieved by modulating the data message with a pseudo-noise (PN) sequence. The detected output signal-to-noise ratio is usually improved by the processing gain, which is specified to be approximately the ratio of the PN sequence waveform bandwidth to the information bandwidth. This processing gain is obtained as a result of the PN property and the narrow chip of the modulating sequence. Unlike DS-SS, the spread bandwidth of the UWB waveform is generated directly and not by modulation with a separate spreading sequence. Thus, UWB is essentially a time-domain concept. The processing gain of UWB is due to the extremely short pulse, which generates a very wide instantaneous bandwidth signal, and is achieved at the receiver by time-gating matched to the pulse duration. The interference suppression is due to the very short time windowing of the interference signal.

This paper is organized as follows. Section II introduces the Gaussian monocycle, its properties and the overall signal model. The UWB performance analysis is developed in section III. Comparison with DS-SS is carried out in section IV. Finally, conclusions are provided in section V.

II. SIGNAL MODEL

The pulse waveform in UWB systems is constrained by FCC regulation 47 CFR Section 15.5(d), which states that “Intentional radiators that produce class B emissions (damped wave) are prohibited”. Various waveforms have been proposed for impulse radio including the Gaussian monocycle [1], the Rayleigh monocycle and the sinusoid monocycle. In general, the goal is to obtain a flat frequency spectrum of the transmitted signal over the bandwidth of the pulse and to avoid a DC component. Unfortunately, all of these practical waveforms have complex mathematical formats unsuitable for closed-form analysis. In [4], we considered a rectangular pulse waveform and obtained closed-form expressions for UWB performance. In this paper, we extend the results of [4] to the Gaussian monocycle. Closed-form expressions are difficult to obtain, but the performance can still be studied by computer-aided numerical analysis.

¹This work was supported in part by the New Jersey Center for Wireless Telecommunications.

Comparing with rectangular waveform, the principal characteristic of the Gaussian monocycle signal is that it has zero DC content to allow it to radiate effectively. The time domain representation of the Gaussian monocycle $p(t; \sigma)$ is [5]:

$$p(t; \sigma) = \left[1 - \left(\frac{t}{\sigma}\right)^2\right] \exp\left[-\frac{t^2}{2\sigma^2}\right], \quad (1)$$

where σ is a pulse width parameter. The effective time duration of the Gaussian monocycle is $T_p = 7\sigma$. This interval contains 99.99 % of the total energy in the Gaussian monocycle. Fig. 1 shows a monocycle with pulse width $T_p = 1$ ns.

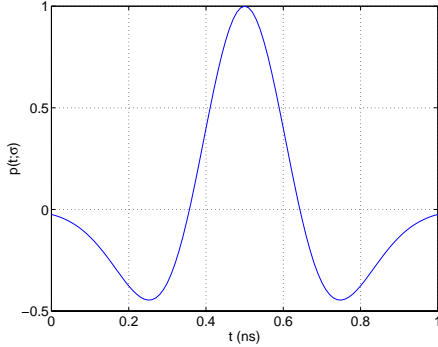


Figure 1: UWB Gaussian monocycle with $T_p = 1$ ns.

The frequency spectrum of the monocycle, $P(f, \sigma)$, is given by [5]:

$$P(f; \sigma) = \sqrt{2\pi\sigma^2} (2\pi\sigma f)^2 \exp\left[-\frac{(2\pi\sigma f)^2}{2}\right] \quad (2)$$

The effective bandwidth is defined as $W = f_H - f_L$, where f_H and f_L are the frequencies measured at the -3 dB emission points. For a given monocycle with pulse width T_p , the corresponding bandwidth W is related to T_p as following:

$$W = \frac{c}{T_p} \quad (3)$$

where c is a constant. In Fig. 2 is shown the frequency spectrum of a Gaussian monocycle in terms of fT_p , with $T_p = 1$ ns. From Fig. 2, we observe that between the 3 dB points, $fT_p = 1.7$, hence the bandwidth is $W = c/T_p = 1.7$ GHz. The analysis in this paper is based on this Gaussian monocycle.

Consider a UWB pulse position modulated and time-hopping communication system. The time-hopping PPM signal for a single user can be written [1]:

$$S(t) = \sum_{j=-\infty}^{\infty} \sqrt{E_p} p(t - jT_f - c_j T_c - d_{[j/N_p]} \delta), \quad (4)$$

where $p(t)$ is the UWB pulse (normalized such that $\int_0^{T_f} p(t)^2 dt = 1$), E_p is the energy per pulse, T_f is the pulse repetition time, the sequence c_j represents the time hopping, with $c_j T_c$ an additional time shift to the j th pulse of the communication burst. For a fixed T_f , the symbol rate $R_s = 1/(N_p T_f)$ determines N_p , the number of pulses that are modulated by a given binary symbol. The information binary sequence $d_{[j/N_p]}$ (e.g. 1000010...) changes at multiples of

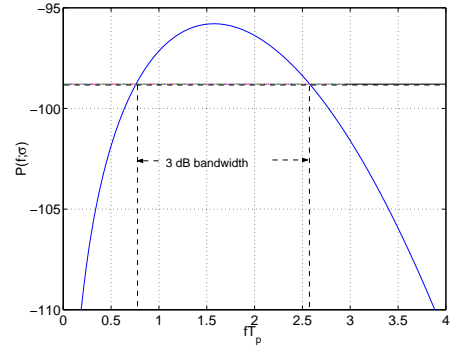


Figure 2: Frequency spectrum of UWB Gaussian monocycle

N_p . The parameter δ is the additional time offset added when $d_{[j/N_p]} = 1$.

The optimal receiver for a single user UWB signal is a pulse correlation receiver. The template waveform used in the correlation receiver is given by

$$v(t) = p(t) - p(t - \delta). \quad (5)$$

For a received signal $R(t) = S(t) + J(t)$, where $J(t)$ is the interference waveform, the correlation receiver computes

$$l_q = \sum_{j=0}^{N_p} \int_{\tau+jT_f}^{\tau+(j+1)T_f} R(t) v(t - jT_f - c_j T_c - \tau), \quad (6)$$

where τ represents the delay with respect to the time origin and $q = [j/N_p]$. Note that we assume perfect synchronization (known τ). Decisions are made according to the rule

$$d_q = \begin{cases} 1 & \text{if } l_q \geq 0 \\ 0 & \text{if } l_q < 0 \end{cases} \quad (7)$$

To simplify the theoretical analysis of jam resistance performance, we make the following additional assumptions:

1. No time-hopping code is used, i.e., $c_j = 0$.
2. To derive the performance of UWB in the presence of interference, we assume 2-PPM symbols. The pulse position time shift for data "1" equals the pulse width, i.e., $\delta = T_p$. Thus the two PPM symbols are $s_1(t) = p(t)$ and $s_2(t) = p(t - T_p)$.
3. The bit interval $T_b = N_p T_f$, implies that one information bit is carried by N_p UWB pulses.
4. The UWB pulse is Gaussian monocycle with temporal and spectral waveform shown in Fig. 1 and Fig. 2, respectively. The monocycle has a pulse duration of $T_p = 1$ ns and a bandwidth of $W = c/T_p$ with $c = 1.7$. Received signals are correlated with the template waveform $v(t)$ shown in Fig. 3.
5. The interference $J(t)$ is modeled as a continuous-time wide sense stationary, random process with the time correlation function $R_J(\tau) = E[J(t)J(t - \tau)]$.
6. System performance is assumed interference limited. The effect of thermal noise is neglected.

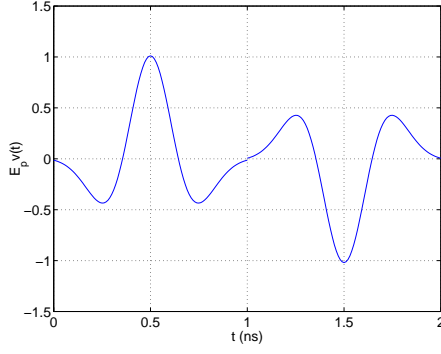


Figure 3: UWB monocycle template waveform.

With those assumptions, the signal received over a bit interval $0 \leq t \leq T_b$, is given by

$$R(t) = \sum_{j=0}^{N_p-1} \sqrt{E_p} p(t - jT_f - dT_p) + J(t), \quad (8)$$

where $d \in \{0, 1\}$ is the information bit.

The cross-correlation $\int_0^{T_f} p(t - dT_p)v(t)dt$ over the pulse interval T_f between the UWB pulse and the template at the receiver is 1 for $d = 0$ and -1 for $d = 1$. Hence, the correlator output for the N_p pulses corresponding to an information bit is given by:

$$\begin{aligned} y(T_b) &= \int_0^{T_b} R(t) \sum_{j=0}^{N_p-1} v(t - jT_f) dt \\ &= \pm \sqrt{E_p} N_p + j(T_b) \end{aligned} \quad (9)$$

where $\pm \sqrt{E_p} N_p$ corresponds to the transmitted information bit '1' and '0', respectively, and $j(T_b)$ represents the interference component.

The interference component at the output of the correlator can be expressed by the functionals v_k :

$$j(T_b) = \int_0^{T_b} J(t) \sum_{k=0}^{N_p-1} v(t - kT_f) dt = \sum_{k=0}^{N_p-1} v_k, \quad (10)$$

where, by definition:

$$v_k = \int_0^{T_f} J(t + kT_f) v(t) dt. \quad (11)$$

The *jam resistance* is determined by the processing gain PG defined as the ratio of the output to the input SIR,

$$PG = \frac{\text{SIR}_{\text{out}}}{\text{SIR}_{\text{in}}} \quad (12)$$

Let the power of a specified interference waveform $J(t)$ at the receiver input be P_J , and the signal power be P_s . The signal power can be expressed $P_s = N_p E_p / T_b$. Then the input SIR is given by

$$\text{SIR}_{\text{in}} = \frac{N_p E_p}{T_b P_J}. \quad (13)$$

The SIR at the output of the UWB correlator receiver depends on the statistical characteristics of both the UWB signal and the interference:

$$\text{SIR}_{\text{out}} = \frac{\{E[y(T_b)]\}^2}{E[j^2(T_b)]} \quad (14)$$

The interference $J(t)$ is modeled by a random process, hence the functionals v_k are random variables. Assuming that the interference is wide-sense stationary, its power at the correlator output is expressed

$$E[j^2(T_b)] = \sum_{n=0}^{N_p-1} \sum_{m=0}^{N_p-1} E[v_n v_m], \quad (15)$$

where the time autocorrelation of the interference samples v_k is given by:

$$\begin{aligned} E[v_n v_m] &= E\left[\int_0^{T_f} J(t + nT_f)v(t)dt \int_0^{T_f} J(t + mT_f)v(t)dt\right] \\ &= \int_0^{T_f} \int_0^{T_f} R_J(t_1 - t_2 + (m - n)T_f) v(t_1)v(t_2) dt_1 dt_2. \end{aligned} \quad (16)$$

III. PERFORMANCE ANALYSIS

The interference signal is modeled with zero mean value ($E[J(t)] = 0$) and constant power spectrum density over the bandwidth W_J :

$$S_J(j\omega) = \begin{cases} \frac{J_0}{2} & |\omega| \leq W_J \\ 0 & \text{otherwise} \end{cases} \quad (17)$$

It follows that the autocorrelation $R_J(\tau)$ is:

$$R_J(\tau) = \frac{J_0}{2} \frac{\sin(2\pi W_J \tau)}{\pi \tau}. \quad (18)$$

Substitute R_J above in (16)

$$\begin{aligned} E[v_n v_m] &= \\ &= \int_0^{T_f} \int_0^{T_f} \frac{J_0}{2} \frac{\sin 2\pi W_J (t_1 - t_2 + (n - m)T_f)}{\pi (t_1 - t_2 + (n - m)T_f)} v(t_1)v(t_2) dt_1 dt_2 \end{aligned} \quad (19)$$

Set $W_J t_1 = t'_1$, $W_J t_2 = t'_2$, $W_J T_p = \alpha$, and $\beta = T_b / T_p$. Then, $E[v_n v_m]$ can be expressed as following:

$$\begin{aligned} E[v_n v_m] &= \\ &= J_0 \int_0^{2\alpha} \int_0^{2\alpha} \frac{\sin 2\pi (t'_1 - t'_2 + \frac{\alpha\beta}{N_p} (n - m))}{2\pi (t'_1 - t'_2 + \frac{\alpha\beta}{N_p} (n - m))} v\left(\frac{t'_1}{W_J}\right) v\left(\frac{t'_2}{W_J}\right) dt'_1 dt'_2 \end{aligned} \quad (20)$$

Use the symbol Θ to express the double integral in the previous expression,

$$E[v_n v_m] = J_0 \Theta^{(n,m)}(\alpha, \beta, N_p)$$

where,

$$\begin{aligned} \Theta^{(n,m)}(\alpha, \beta, N_p) &= \\ &= \int_0^{2\alpha} \int_0^{2\alpha} \frac{\sin 2\pi (t'_1 - t'_2 + \frac{\alpha\beta}{N_p} (n - m))}{2\pi (t'_1 - t'_2 + \frac{\alpha\beta}{N_p} (n - m))} v\left(\frac{t'_1}{W_J}\right) v\left(\frac{t'_2}{W_J}\right) dt'_1 dt'_2 \end{aligned} \quad (21)$$

Then (15) can be expressed

$$E[j^2(T_b)] = J_0 \sum_{n=0}^{N_p-1} \sum_{m=0}^{N_p-1} \Theta^{(n,m)}(\alpha, \beta, N_p) \quad (22)$$

Since $E[J(t)] = 0$, clearly, mean value of the interference component $j(T_b)$ is $E[j(T_b)] = 0$. From (14) and (22), the output SIR at the receiver is:

$$\text{SIR}_{\text{out}} = \frac{N_p^2 E_p}{J_0 \sum_{n=0}^{N_p-1} \sum_{m=0}^{N_p-1} \Theta^{(n,m)}(\alpha, \beta, N_p)} \quad (23)$$

With $J_0 = P_J/W_J$ and $P_s = N_p E_p/T_b$, finally, we have

$$\text{SIR}_{\text{out}} = \frac{P_s}{P_J} \frac{\alpha\beta}{\Psi(\alpha, \beta, N_p)} \quad (24)$$

$$= \text{SIR}_{\text{in}} \frac{\alpha\beta}{\Psi(\alpha, \beta, N_p)} \quad (25)$$

where:

$$\Psi(\alpha, \beta, N_p) = \frac{1}{N_p} \sum_{n=0}^{N_p-1} \sum_{m=0}^{N_p-1} \Theta^{(n,m)}(\alpha, \beta, N_p) \quad (26)$$

and $\Theta^{(n,m)}(\alpha, \beta, N_p)$ is the quantity defined in (21).

According to (12) and (25), the processing gain of UWB with Gaussian monocycle is PG_{mono} , given by:

$$\text{PG}_{\text{mono}} = \frac{\alpha\beta}{\Psi(\alpha, \beta, N_p)} \quad (27)$$

We previously defined $\alpha = W_J T_p$. According to (3), α can be written as:

$$\alpha = W_J T_p = c \frac{W_J}{W} \quad (28)$$

For a certain UWB system with pulse width T_p , c is constant. Thus α serves as a measure of comparative bandwidth between the interference and UWB system. Specifically, $\alpha \rightarrow \infty$ corresponds to an interference bandwidth much larger than that of the UWB signal, and $\alpha \rightarrow 0$ represents a narrowband interference. In [4], the close-form approximation for $\alpha \rightarrow \infty$ and $\alpha \rightarrow 0$ were developed for rectangular pulse waveform. Even though it is impossible to deduce such approximation for Gaussian monocycle waveform, we can get some conclusion by comparing the jam resistance between rectangular and Gaussian monocycle waveform.

Define G as the ratio of the processing gain for the different pulse waveform. Recall the processing gain for rectangular pulse in [4], which is referred as PG_{re} , as following:

$$\text{PG}_{\text{re}} = \frac{\alpha\beta}{\Phi(\alpha, \beta, N_p)}, \quad (29)$$

where $\Phi(\alpha, \beta, N_p)$ is the factor defined in [4]. The variables α , β and N_p have the same significance as in this paper.

Then from (27) and (29), we obtain

$$G = \frac{\text{PG}_{\text{mono}}}{\text{PG}_{\text{re}}} = \frac{\Phi(\alpha, \beta, N_p)}{\Psi(\alpha, \beta, N_p)} \quad (30)$$

This factor measures the interference suppression capability of Gaussian monocycle relative to that of rectangular pulse. As demonstrated by Fig. 4, when $\alpha \gg 1$, $G = 1$, so for two UWB system have the same interference suppression. Further we can get the approximation for Gaussian monocycle when $\alpha \gg 1$ as following[4]:

$$\text{PG}_{\text{mono}}(\alpha \rightarrow \infty) = \text{PG}_{\text{re}}(\alpha \rightarrow \infty) \simeq \alpha\beta. \quad (31)$$

Above result shows that when the interference bandwidth is larger than the UWB system bandwidth, the processing gain

is a linear function of α and β . This result can be explained as follows:

(1) As α increases, the interference bandwidth increases and more of the interference power is outside the receiver bandwidth. Thus an increase in α causes a decrease in the interference component.

(2) For fixed T_p , as $\beta = T_b/T_p$ increases so does the bit interval, T_b . For a fixed transmitted power P_s , this means an increase in the energy per bit E_b . In this case, the interference resistance increase is due to the increase in the output signal power.

The more interesting case is when $\alpha \ll 1$, interference bandwidth is much smaller than UWB signal. Fig. 4 demonstrates the higher jam resistance ability of UWB system with Gaussian monocycle to narrowband interference than rectangular pulse. This result can be explained by the interference reduction mechanism through time windowing. Unlike the rectangular pulse in [4] which is non-negative, the Gaussian monocycle in Fig. 1 has two zero-crossing points. This results in subtraction of highly correlated interference components and hence it leads to interference suppression. This effect causes the advantage of Gaussian monocycle to suppress narrowband interference.

IV. COMPARISON OF UWB AND DS-SS

Communications utilizing UWB and DS-SS signals are similar in the sense that both use a short pulse (PN chip in DS-SS) to get the spread spectrum effect. But, there are fundamental differences between the two systems. The UWB system works at baseband and the pulses emitted by the transmitter are discontinuous. Conversely, DS-SS signals are continuous and with an information waveform modulated by a spread spectrum waveform and a carrier frequency.

Traditional DS-SS has a constant envelope with a 100% duty cycle and a peak power P_{peak} equal to the average power P_s . With UWB, the pulse duration is extremely short with respect to the pulse repetition time resulting in pulse peak powers hundreds of time larger than the average power. To compare the performance of UWB and DS-SS, assume that they have the same average power P_s (average power constraint), the same bit interval T_b and that both are subject to an interference with average power P_J . Performance is assumed interference limited, hence the effect of additive white Gaussian noise is neglected. As the two systems have the same input SIR, performance can be compared based only on the output SIR.

Furthermore, in typical applications, the chip width of DS-SS will be much larger than the UWB pulse width. Hence, the same interference with a certain bandwidth W_J , could be narrowband with respect to UWB and wideband with respect to DS-SS. For UWB, the parameter α was defined as pulse width \times interference bandwidth. This definition can be extended to DS-SS, where the pulse width is the chip time T_c , hence for DS-SS, $\alpha = W_J T_c$. Thus α serves as a measure of comparative bandwidth between the interference and either system. It is of interest to compare the performance of the two systems in the presence of interference. Notably, the mechanisms for interference suppression are quite different. With DS-SS, the interference is typically spread by cross-correlation with the PN sequence and is subsequently reduced by lowpass filtering at the data bandwidth. In contrast, with UWB there are two mechanisms for interference suppression: (1) the receiver is a

filter matched to the transmitted UWB signal - this suppression mechanism applies to wideband interference (bandwidth larger than UWB signal), (2) a narrowband interference is highly correlated over the time δ used in (5), resulting in interference suppression.

To proceed with the comparison between UWB and DS-SS, consider a DS-SS system utilizing binary PSK, with a bit interval T_b , chip interval T_c , and $L_c = T_b/T_c$. Here we assume the bit energy of DS-SS is same as that of UWB, e.g. $E_b = N_p E_p$. Thus DS-SS and UWB have the same input SIR as defined in (13)

From [6], the output SIR of DS-SS in the presence of an interference with power spectrum density defined in (17) is given by:

$$\text{SIR}_{\text{out}} = \frac{2E_b}{J_0 I(\alpha)}, \quad (32)$$

where:

$$I(\alpha) = \int_{-\alpha}^{\alpha} \left(1 - \frac{|x|}{\alpha}\right) \frac{\sin \pi x}{\pi x} dx. \quad (33)$$

It is easy to show that the processing gain of DS-SS, PG_{DSSS} is:

$$\text{PG}_{\text{DSSS}} = \frac{2\alpha L_c}{I(\alpha)}. \quad (34)$$

Let both systems have the same information bandwidth spreading, viz., $\beta = T_b/T_p = L_c$. Define the gap of DS-SS to UWB as the ratio of processing gain, it follows that for UWB utilizing Gaussian monocycle,

$$G = \frac{\text{PG}_{\text{mono}}}{\text{PG}_{\text{DSSS}}} = \frac{I(\alpha)}{2\Phi(\alpha, \beta, N_p)}. \quad (35)$$

and for rectangular pulse,

$$G = \frac{\text{PG}_{\text{re}}}{\text{PG}_{\text{DSSS}}} = \frac{I(\alpha)}{2\Phi(\alpha, \beta, N_p)}. \quad (36)$$

This factor measures the interference suppression capability of UWB relative to DS-SS. As shown in Fig. 4, when $\alpha \gg 1$, for wideband interference, the value of G is equal to -3dB. This is because in DS-SS binary PSK, the two signals are antipodal, while the PPM UWB signals are orthogonal. Inherently, an antipodal constellation has a 3 dB signal-to-noise ratio advantage over an orthogonal modulation. We conclude that, except for this 3dB difference caused by the different modulation format, for wideband interference both systems have similar interference suppression capability.

As for narrowband interference, $\alpha \rightarrow 0$, Thus for narrowband interference (compared to the spread spectrum bandwidth), the advantage of UWB increases dramatically with $1/\alpha$. This is a significant result as this is the likely region of operation for UWB. In this region, UWB is superior to DS-SS. This is also demonstrated by the plot of the gap G versus α in Fig. 4. For example, for an integration of $N_p = 1$ UWB pulses and $\beta = 100$, at $\alpha = 0.1$ (interference bandwidth approximately 10% of spread spectrum bandwidth), UWB utilizing Gaussian monocycle has more than 40 dB advantage in interference suppression over DS-SS. While for UWB utilizing rectangular pulse, jam resistance ability is reduced, but it still has 4 dB advantage over DS-SS.

V. CONCLUSIONS

We analyzed the performance of UWB communications in presence interference. Mathematical expressions are developed for the jam resistance of a pulse position modulation

UWB utilizing Gaussian monocycle. The performance comparison between Gaussian monocycle and rectangular pulse is developed. The comparison between the interference suppression capability of UWB and DS-SS shows that for wideband interference (interference bandwidth exceeds spread spectrum bandwidth) the performance of the two system is similar. The more practical situation is, however, a narrowband interference affecting the communication link. In this case, we have shown that UWB has a much better ability than DS-SS to suppress interference.

References

- [1] R.A. Scholtz, "Multiple access with time-hopping impulse modulation," *Proceeding of IEEE MILCOM '93*, vol. 3, Oct. 1993.
- [2] M.Z. Win, *Ultra-wide Bandwidth Spread-Spectrum Techniques for Wireless Multiple-Access Communications*, Ph.D. thesis, Electrical Engineering, University of Southern California, Los Angeles, CA., Jan. 1998.
- [3] G.D. Weeks, J.K. Townsend, and J.A. Freebersyser, "Quantifying the covertness of pulse radio," *1999 International UWB Conference*, Sep. 1999.
- [4] L. Zhao and A.M. Haimovich, "Performance of ultra-wideband communications in the presence of interference," *Accepted by IEEE ICC*, 2001, Helsinki, Finland.
- [5] J.T. Conroy, J.L. LoCicero, and D.R. Ucci, "Communication techniques using monopulse waveforms," *Proceeding of IEEE MILCOM' 99*, vol. 2, pp. 1191-1185, 1999.
- [6] J.G. Proakis and M. Salehi, *Communication Systems Engineering*, Prentice Hall, 1994.

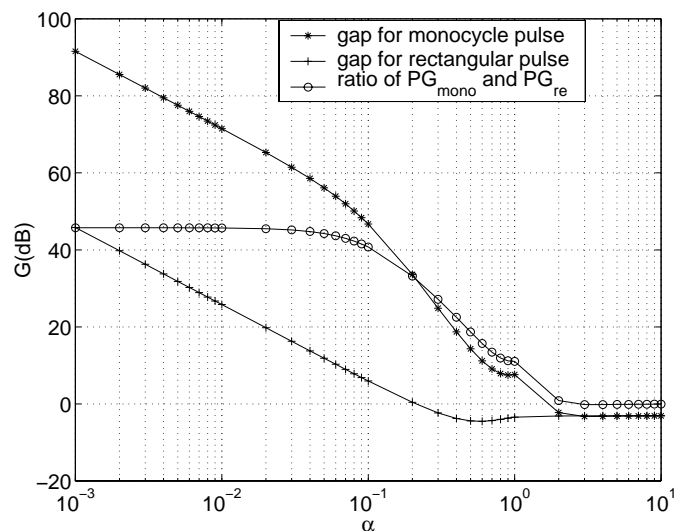


Figure 4: Advantage of UWB with respect to DS-SS as a function of α